Cancer Letters 595 (2024) 216985

Contents lists available at ScienceDirect

Cancer Letters

journal homepage: www.elsevier.com/locate/canlet

Original Articles

Colorectal cancer-associated fibroblasts inhibit effector T cells via NECTIN2 signaling

David J. Agorku [a,b], Andreas Bosio [a], Frauke Alves [c,d,e], Philipp Ströbel [b], Olaf Hardt [a,*]

[a] Miltenyi Biotec B.V. & Co. KG, Bergisch Gladbach, Germany
[b] University Medical Center Göttingen (UMG), Institute of Pathology, Göttingen, Lower Saxony, Germany
[c] University Medical Center Göttingen, Department of Hematology and Medical Oncology, Göttingen, Lower Saxony, Germany
[d] University Medical Center Göttingen, Institute for Diagnostic and Interventional Radiology, Göttingen, Lower Saxony, Germany
[e] Max Planck Institute for Multidisciplinary Sciences, Translational Molecular Imaging, Göttingen, Lower Saxony, Germany

ARTICLE INFO

Keywords:
Colorectal cancer
Cancer-associated fibroblasts
Fibroblast heterogeneity
NECTIN2
TinCAFs

ABSTRACT

Cancer-associated fibroblasts play a crucial role within the tumor microenvironment. However, a comprehensive characterization of CAF in colorectal cancer (CRC) is still missing. We combined scRNA-seq and spatial proteomics to decipher fibroblast heterogeneity in healthy human colon and CRC at high resolution. Analyzing nearly 23,000 fibroblasts, we identified 11 distinct clusters and verified them by spatial proteomics. Four clusters, consisting of myofibroblastic CAF (myCAF)-like, inflammatory CAF (iCAF)-like and proliferating fibroblasts as well as a novel cluster, which we named "T cell-inhibiting CAF" (TinCAF), were primarily found in CRC. This new cluster was characterized by the expression of immune-interacting receptors and ligands, including CD40 and NECTIN2. Co-culture of CAF and T cells resulted in a reduction of the effector T cell compartment, impaired proliferation, and increased exhaustion. By blocking its receptor interaction, we demonstrated that NECTIN2 was the key driver of T cell inhibition. Analysis of clinical datasets showed that *NECTIN2* expression is a poor prognostic factor in CRC and other tumors.

In conclusion, we identified a new class of immuno-suppressive CAF with features rendering them a potential target for future immunotherapies.

1. Introduction

Colorectal cancer (CRC) is among the most frequent and fatal cancers, causing many cancer-related deaths. In 2020, it was the 3rd most common cancer, accounting for 10 % of the new diagnoses, while causing 9.4 % of all cancer-related deaths [1]. Although surgical resection and chemotherapy have proven effective in many cases, immunotherapy is a promising approach for high-risk patients that make up to 20 % of all cases in CRC.

Detailed analysis of CRC has shown a heterogeneous tumor microenvironment with a distinctive population of fibroblasts [2]. Several aspects of tumor growth and progression have been associated with cancer-associated fibroblasts (CAF) [3,4]. It has been reported that CAF regulate the recruitment of inflammatory cells [5], and affect angiogenesis, tumor stemness and drug resistance [6,7]. Thus, CAF substantially contribute to cancer progression and are considered an essential target for therapy.

Fibroblasts represent a highly plastic cell type with various functions and activation states [8]. Multiple markers have been used to discriminate them within the tumor microenvironment (TME), including α-smooth muscle actin, fibroblast-activated protein (FAP), S100A4 and platelet-derived growth factor α and β-receptor [9–11]. Various attempts have been made to eradicate fibroblasts in cancer to remove their tumor-promoting functions. Surprisingly, in pancreatic ductal adenocarcinoma (PDAC) and CRC, ablation of fibroblasts either by genetic engineering in mouse models or immunotherapeutic targeting resulted in poorer outcomes and showed unfavorable effects [12–15]. The identification of functionally distinct subtypes of CAF in PDAC, such as myofibroblastic CAF (myCAF), inflammatory CAF (iCAF), and antigen-presenting (apCAF), offers possible explanations for these results as not all subpopulations of CAF are equally pro-tumorigenic [15–18]. A better understanding of distinct fibroblast subpopulations offers the opportunity to specifically eradicate tumor-promoting CAF to improve the outcome of targeted tumor therapies [7].

* Corresponding author.
E-mail address: olaf@miltenyi.com (O. Hardt).

https://doi.org/10.1016/j.canlet.2024.216985
Received 8 March 2024; Received in revised form 29 April 2024; Accepted 23 May 2024
Available online 29 May 2024

Despite advances in the characterization of CAF in PDAC [16–19], breast cancer [20,21], and lung cancer [22], a comprehensive analysis of colorectal CAF is still missing. So far, two principal CAF subtypes have been described [23,24] either expressing extracellular matrix (ECM) molecules and modulators (termed CAF-A) or resembling myofibroblastic CAF (termed CAF-B) [24]. In addition, CRC CAF signatures have been correlated with poor prognosis [25]. However, as previous studies have focused on analyzing the overall cellular composition of CRC, extensive analysis of CAF subtypes was hampered by relatively low numbers of sequenced CAF, usually in the range of 30–800 cells [23,24]. Summarizing the available studies, it was demonstrated that CAF play a central role in CRC, yet, a comprehensive analysis of CAF heterogeneity is still missing.

In this study, we performed an in-depth analysis of fibroblast heterogeneity in human colon and CRC tissue samples by combining single-cell RNA sequencing (scRNA seq) and spatial proteomics. We identified 11 distinct fibroblast clusters with different functional traits. Moreover, we show that four of the identified subtypes are cancer-associated and that those are preferentially found close to T cells in the TME rather than close to cancer cells. Finally, we demonstrate that one of these clusters, which we named TinCAF, represents a novel subtype which can suppress T cell proliferation and effector functionality while increasing exhaustion via NECTIN2 and CD40 signaling. Analyzing clinical datasets, we found that high expression of markers characteristic for TinCAF is associated with reduced relapse-free survival in CRC patients. Hence, this newly identified class of CAF might represent a potential target for future immunotherapies in CRC.

2. Materials and methods

2.1. Fibroblast isolation for single-cell sequencing

Primary human CRC and normal tissue samples were collected at the University Medical Center Göttingen from CRC patients undergoing surgical resection of tumor masses (clinical characteristics are summarized in Supplementary Table 2). The tissue was stored in MACS Tissue Storage Solution before dissociation using the Tumor Dissociation Kit, human in combination with the gentleMACS™ Octo Dissociator with Heaters (all Miltenyi Biotec) according to the manufacturer's instructions. Fibroblasts from normal adjacent or cancer tissue were isolated by magnetic activated cell sorting (MACS)-based depletion of cells expressing GlyA, CD45, CD31 or EPCAM. Single-cell suspensions were labeled with respective MicroBeads and depleted via LS columns (all Miltenyi Biotec). The isolation procedure was performed according to the manufacturer's instructions. Purity and yield were assessed by flow cytometric analysis using fluorochrome-conjugated antibodies against CD90, CD31, CD45, CD326, and GlyA on a MACSQuant Analyzer 16 (all Miltenyi Biotec). Isolated cells were immediately cryopreserved in MACS Freezing Solution (Miltenyi Biotec) and stored in liquid nitrogen until all samples were collected.

For the library generation, cells were thawed at 37 °C in a water bath and immediately transferred to pre-warmed Colon TumorMACS™ (Miltenyi Biotec) supplemented with 8 % FBS (Catus Biotech) and centrifuged at 300 *g* for 5 min. After removing the supernatant, the cells were carefully washed two times with PBS (Ca^{2+}- and Mg^{2+}-free; Lonza) supplemented with 0.04 % BSA. The pellet was resuspended in PBS (Ca^{2+}- and Mg^{2+}-free; Lonza) supplemented with 0.04 % BSA again and counted using the Countess™ cell counter (Invitrogen). The cell concentration was adjusted to 800–1000 cells/μL.

2.2. Single-cell RNA sequencing

To prepare the scRNA seq libraries, the Chromium Next GEM Single Cell 5′ Library and Gel Bead Kits v1.1 were used according to the manufacturer's instructions (10× Genomics). The single-cell gel beads in emulsions (GEMs) were prepared on a Chromium Single-Cell Controller Instrument (10× Genomics), aiming to capture 10,000 cells per library. GEM generation was followed by reverse transcription, disruption of GEMs, and cDNA clean-up. Next, the cDNA was PCR-amplified, followed by sequencing the libraries with a NextSeq 550 High Output Kit v2.5 (150 Cycles) on a NextSeq 550 platform (Illumina).

2.3. scRNA seq clustering, cluster analysis and gene set enrichment analysis of cancer hallmarks

By using CellRanger (version 6.1.2), the raw data were demultiplexed, and the reads were mapped to the transcriptome. The resulting raw unique molecular identifier (UMI) count matrix was converted into a Seurat object by the R package Seurat (version 4.3.0) [26]. Single cells with <200 or >3500 genes, with >75,000 read counts, or with >12.5 % of reads mapping to mitochondrial RNA were excluded for each object individually. Next, using the *merge* function all Seurat objects were merged and integrated to generate one aggregated object. Cells were normalized and scaled (*ScaleData*). Dimensionality was assessed and the Principal Components (PCs) covering the highest variance in the aggregated dataset were chosen for the graph-based clustering. Clustering was performed using the *FindNeighbors* and *FindClusters* functions in Seurat. Clusters were visualized with the dimensional reduction method UMAP (*Uniform Manifold Approximation and Projection*) in Seurat. The remaining contaminating immune, epithelial, and neural cell clusters were identified based on marker genes in violin plots. The corresponding clusters were removed via the *subset* function, followed by scaling and clustering the remaining cells again. To identify differentially expressed genes, the *FindAllMarkers* function was used with default settings (Seurat version 4.3.0; *Wilcoxon Rank Sum test; logfc. threshold = 0.25; min. pct = 0.1*). Gene set enrichment analysis was performed using the R package fgsea (version 1.24.0). For this, all differentially expressed markers were passed to the function, and different lists of genes were analyzed.

2.4. Spatial proteomic analysis

Primary human CRC and normal adjacent tissues were collected at the University Medical Center Göttingen from patients undergoing surgical resection of tumor masses (see above). Tissue samples for MICS analysis were fixed in 4 % paraformaldehyde for 2 h, washed in 30 % sucrose solution overnight to prevent the formation of ice crystals during freezing, embedded in Tissue Freezing Medium (Leica) and snap-frozen and stored at −70 °C until use. For proteomic analysis, 8 μm cryosections were cut on a CM3050 S cryostat (Leica), collected on SuperFrost® Plus slides (Menzel) and stored at −70 °C. On the day of use, the sections were taken out of the −70 °C storage and the MACSwell™ Four Imaging Frame was immediately mounted on the slide. The section was then washed with MACSima Running Buffer (Miltenyi Biotec), pre-stained with DAPI (Miltenyi Biotec), and transferred to the MACSima™ Imaging Platform (Miltenyi Biotec). The MACSima™ Imaging System combines liquid handling with widefield microscopy for fully automated cyclic immunofluorescence imaging. In brief, each staining cycle consisted of the immunofluorescent antibody staining, sample washing, image acquisition, and signal erasure (photobleaching in this case). Images were generated according to the manufacturer's instructions and analyzed using MACSiQView software (version 1.1.0 Miltenyi Biotec). Details of the antibodies used can be found in the Supplementary Table 1.

For assessment of fluorescence intensities, cell segmentation was done by choosing nuclear and cytoplasma segmentation in the software using *constrained doughnut* method. Fibroblasts were identified by exclusion of cells expressing non-fibroblast markers (see Supplementary Fig. 4B). Fluorescence intensities ("*CellExp*") for the different markers expressed by fibroblasts were exported using the *export* function of the *Feature Table*. To define fibroblast populations dependent on distance to other cell populations, *distance metrics* were generated via the *Workflow*

Editor and fibroblasts were plotted against the distance metrics (see Supplementary Fig. 4D). "Close" and "distant" fibroblasts were then gated accordingly (Supplementary Fig. 4D) and the fluorescence intensities were exported as described above.

2.5. Primary fibroblast culture

Fibroblast cultures were generated from isolated fibroblasts (see above). After MACS-based isolation, fibroblasts were plated in Colon TumorMACS™ medium (Miltenyi Biotec) supplemented with 8 % FBS (Catus Biotech). Cells were maintained at 37 °C in a humidified 9 % CO_2 atmosphere. Cells were passaged when they reached a confluency of approx. 80–90 % using 0.25 % Trypsin/EDTA (Sigma Aldrich) and re-seeded at 5×10^4 cells/cm^2 density. Of note, primary fibroblasts were used only until passage 10.

The choice for Colon TumorMACS™ medium supplemented with FBS for maintaining primary CAFs was based on empirical data (data not shown). We observed efficient growth of CAFs in this medium in the absence of FBS in primary patient-derived cancer cell cultures, resulting in heterogenous cultures. However, isolated CAFs required the addition of FBS for plating and expansion. In addition, the widely used CAF-medium DMEM supplemented with FBS was tested for propagation of primary CAFs, but this resulted in reduced heterogeneity of CAFs and a rapid polarization towards the myofibroblastic phenotype within 1–2 passages compared to TumorMACS medium, which was able to maintain a level of CAF heterogeneity until at least passage 10.

2.6. T cell isolation

Peripheral blood mononuclear cells (PBMCs) were isolated from whole blood donations of healthy anonymous donors (Miltenyi Biotec) by density gradient centrifugation. T cells were purified from PBMCs using the Pan T Cell Isolation Kit, human (Miltenyi Biotec), according to the manufacturer's instructions.

2.7. CAF – T cell co-culture assay

CAF were harvested a day before the co-culture and seeded in Colon TumorMACS™ medium (Miltenyi Biotec) supplemented with 8 % FBS (Catus Biotech) overnight. The next day, T cells were isolated as described above. To analyze T cell proliferation, freshly isolated T cells were stained with CellTrace™ Violet (Invitrogen™). In brief, cells were washed with PBS after isolation and incubated with 5 μM CellTrace Violet at 37 °C for 20 min. Then, TexMACS medium (Miltenyi Biotec) was added, cells were incubated for an additional 5 min at room temperature, centrifuged at 300 *g* for 5 min, and then resuspended in TexMACS medium supplemented with 200 IU/mL IL-2 (both Miltenyi Biotec). The cells were analyzed using the MACSQuant Analyzer 16 (Miltenyi Biotec). The medium from the CAF overnight cultures was removed, and stained T cells were then added to the CAF at a 2:1 ratio. Cells were co-cultured for 72 h in the absence or presence of the CD3$^-$and CD28-cross-linking reagent TransAct (Miltenyi Biotec) for T cell stimulation, before they were harvested and analyzed by flow cytometry.

2.8. Blocking experiments

To assess the function of NECTIN2 or CD40 expressed on fibroblasts, fibroblasts were seeded for co-culture assays as described above. One hour prior to adding T cells as described above, NECTIN2- or CD40-blocking antibody was added to the fibroblast cultures at a concentration of 7.5 μg/mL and incubated at 37 °C and 9 % CO_2 until addition of T cells. The co-cultures were set up and maintained as described above.

2.9. Flow cytometric analysis

For flow cytometric analysis, single-cell suspensions were stained with the indicated antibodies (Supplementary Table S1) according to the manufacturer's instructions and analyzed using the MACSQuant™ Analyzer 16 (Miltenyi Biotec). Briefly, cells were stained at a density of $0.5–2 \times 10^5$ cells per sample in 50 μL volume of PBS pH 7.2, 2 mM EDTA, and 0.5 % BSA (PEB) buffer at 2–8 °C for 10 min, followed by a washing step with PEB. Cell viability was assessed by Propidium Iodide (PI, 1 μg/mL, Miltenyi Biotec) which was added prior to flow cytometric analysis. Analysis was performed using the MACSQuant Analyzer 16, and data were analyzed using the MACSQuatify software (Miltenyi Biotec).

2.10. Analysis of clinical data

To evaluate the prognostic value of candidate genes, the publicly available Kaplan-Meier Plotter (http://kmplot.com/analysis/) was used. The Kaplan-Meier survival plots of the two patient cohorts were compared using a logrank test with hazard ratios (HRs) and 95 % confidence intervals [27].

2.11. Statistical analysis

Unless otherwise specified, all graphs show the mean with error bars representing the standard error of the mean. Statistical comparisons between two groups were conducted by paired *t*-Test with *P*-value <0.05 using GraphPad Prism 9. Statistical comparisons between more than two groups were conducted by two-way ANOVA with *P*-value <0.05 using GraphPad Prism 9. For co-culture experiments, at least $n = 3$ wells were analyzed, and experiments were independently repeated at least twice.

2.12. Ethical concerns

For all studies using anonymized human primary tissue, written informed patient consent was obtained with approval of the Ethical committee of the University Medical Center Göttingen (#25/8/15). Peripheral blood mononuclear cells (PBMCs) were isolated from whole blood of healthy anonymous volunteers who gave their written consent before. All blood samples were handled following the required ethical and safety procedures.

3. Results

3.1. High resolution scRNA seq reveals CAF heterogeneity

To allow for a comprehensive analysis of fibroblast heterogeneity at high resolution, fibroblasts were enriched from tissue biopsies by a magnetic-based cell isolation after tissue dissociation (Fig. 1a and b). This allowed for subsequent deep analysis of pure fibroblast populations from both normal colon tissue from colon cancer patients (in the following referred to as "normal") and cancer tissue by single-cell RNA sequencing (Fig. 1c and d). After quality control and aggregation of fibroblasts from eight different samples (6 CRC, 2 normal colon samples; Supplementary Figs. 1a–f), the transcriptomes of 22,865 single fibroblasts were analyzed. The cells clustered into eleven distinct clusters (Fig. 1c). Interestingly, most clusters were found in both normal samples and CRC tissue (Fig. 1d; Supplementary Figs. 1g and 2). However, clusters 3, 5, 7 and 9, were almost exclusively found in CRC tissue but absent among normal tissue-associated fibroblasts (NF), accordingly representing CAF specific clusters.

Based on the analysis of differentially expressed marker genes, known fibroblast subtypes such as apCAF (cluster 1; *HLA-DRA* and *CD74* expression), "epithelial maintenance" fibroblasts (cluster 2; *SOX6* and *POSTN* expression), myCAF (cluster 3; *MUSTN1* and *ACTA2* expression) and iCAF (cluster 7; *IL6* expression) were identified (Fig. 1e). Cluster 9 showed high expression of *MKI67*, *CENPF*, *CDK1* and further cell cycle-

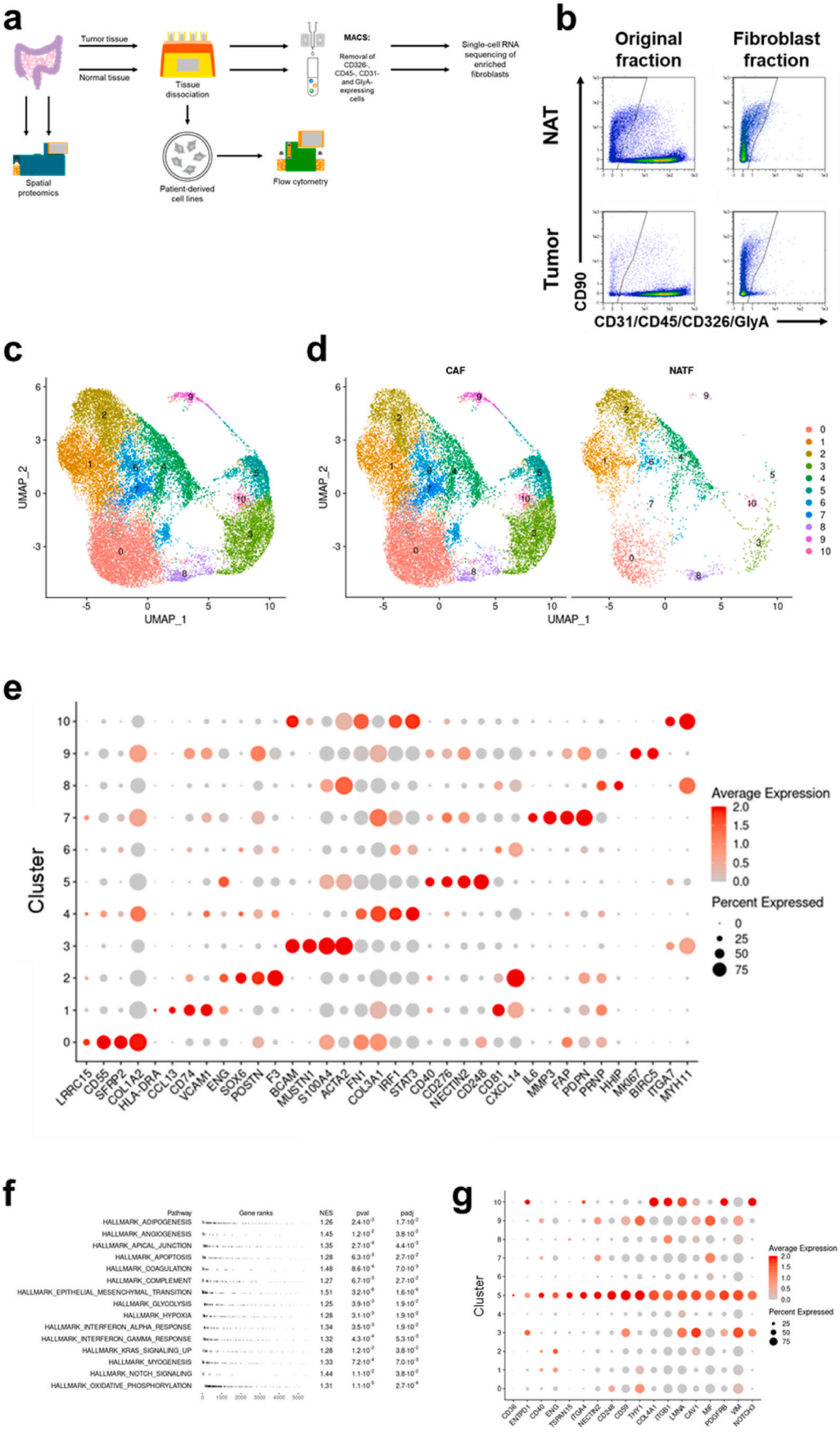

(caption on next page)

Fig. 1. Fibroblast heterogeneity in CRC and colon at the transcriptomic level.
a Workflow for processing colon tissue samples. **b** Representative data for magnetic isolation of fibroblasts from normal adjacent tissue (NAT, upper panel) and CRC tissue (Tumor, lower panel). **c** UMAP (Uniform Manifold Approximation and Projection) plot of 11 distinct fibroblast clusters revealed by scRNA seq analysis. **d** Cluster abundance among CAF and NATFs. **e** Dotplot representation of differentially expressed marker genes for each fibroblast cluster. The size of the dots represents the percentage of fibroblasts expressing the respective gene, the color indicates the average expression level. **f** GSEA analysis of cancer hallmarks for cluster 5 CAF. **g** Overview of genes highly expressed by cluster 5 CAF.

associated genes, identifying this cluster as the compartment of proliferating fibroblasts. Cluster 5 did not express known CAF-characteristic markers. This newly identified cluster of CAF showed expression of immune-associated genes such as *CD40*, *CD276*, and *NECTIN2* (Fig. 1e). In summary, our results demonstrated fibroblast heterogeneity in the human normal colon tissue and CRC tissue, revealing known CAF subtypes but identified a new cluster of CAF.

3.2. The newly identified cluster of CAF shows interferon response- and immune-modulation traits

To further analyze cluster 5 and its potential functional characteristics, we utilized gene set enrichment analysis (GSEA). Enriched gene sets in cluster 5 were associated with the interferon response and oxidative phosphorylation, indicating that these CAF were immune responsive and metabolically active (Fig. 1f). When assessing further differentially expressed genes in cluster 5, we noticed additional genes that were associated with immune modulation such as *ENTPD1* (CD39), *CD59*, *CAV1*, *MIF* and *Notch3* (Fig. 1g). In conclusion, we found that cluster 5 fibroblasts were cancer-associated, but distinct from known CAF subsets and showed an immune-modulatory gene expression profile.

3.3. Spatial proteomic analysis shows expression of NECTIN2 on fibroblasts but not on tumor cells

To analyze fibroblast heterogeneity at the proteomic level and to characterize their spatial distribution at single-cell resolution, we used MACSima® Imaging Cyclic Staining (MICS) technology [28]. We analyzed CRC and normal tissue samples using antibodies specific for proteins corresponding to characteristic genes identified by scRNA seq. We identified fibroblast subpopulations recapitulating the clusters revealed by scRNA seq in human CRC (Fig. 2a, Supplementary Fig. 3a) and normal tissue (Supplementary Figs. 3b and c).

When comparing the level of protein expression of cluster-characteristic markers in fibroblasts in CRC and normal tissue of the same patient, we saw differential expression, confirming fibroblast heterogeneity and CAF-specific signatures at the proteomic level (Fig. 2b). Of note, we analyzed normal tissue corresponding to the matched tumor samples. Accordingly, it could be subject to paracrine signaling from the tumor and thus show altered expression for the analyzed markers. As the newly identified cluster 5 was of particular interest, we analyzed the expression of the cluster 5 protein marker NECTIN2 (CD112) more closely. NECTIN2 expression was found exclusively in the tumor microenvironment, where it primarily co-localized with a subpopulation of CD90-expressing fibroblasts, but not on epithelial tumor cells (Fig. 2c).

Taken together, we confirmed fibroblast heterogeneity at the proteomic level. Moreover, NECTIN2 was primarily found on CAF but not on tumor cells, as seen by the co-localization with CD90 but not EPCAM.

3.4. Spatial analysis of CAF-related marker proteins shows increased expression in CAF close to T cells

We investigated the spatial distribution of the identified CAF clusters (Supplementary Figs. 4 and 5). The scRNA seq data suggested clusters 3, 5 and 7 to be cancer-associated as they were almost exclusively identified among the CRC samples. Accordingly, we expected a close association of the CAF cluster protein markers with epithelial tumor cells. Surprisingly, we found that CAF marker expression was significantly higher in fibroblasts distant from $EPCAM^+$ cells (≥approx. 15 μm), except for FAP expression (Fig. 3a). Since cluster 5 was associated with immune- and T cell-interaction traits, we analyzed the expression patterns of CAF marker proteins in relation to T cells (Fig. 3b). All CAF-associated markers were expressed at significantly higher levels in fibroblasts that were close to T cells. These findings point to a close interaction between T cells and CAF and raise the possibility that T cells could affect the recruitment and distribution of certain CAF in the TME.

3.5. CRC CAF suppress T cell proliferation and activation

Our spatial proteomics analysis suggested a close interaction between CAF and tumor-infiltrating T cells. We, therefore, evaluated the effects of colorectal cancer-derived CAF on T cells using co-culture assays. Since the new CAF cluster 5 showed the most immune-interacting traits, we first asked whether this cluster was preserved upon *in vitro* propagation of primary CAF isolated from CRC tissue. Six characteristic protein markers for cluster 5 CAF could be detected in primary CAF cultures from different patients using flow cytometry (Fig. 4a and b) and co-expression was confirmed (Fig. 4c), suggesting that the phenotype of cluster 5 CAF was maintained in primary culture.

To characterize interactions between CAF and T cells, primary CAF were co-cultured with T cells for three days (Fig. 4d). T cells were stimulated via CD3 and CD28 cross-linking (using TransAct) during co-culture to simulate activation. Despite constant T cell stimulation throughout the co-culture, CAF significantly decreased T cell viability and proliferation, demonstrating the T cell suppressive properties of CRC CAF (Fig. 4e). T cells were additionally analyzed for activation and inhibitory/exhaustion markers by flow cytometry (Supplementary Fig. 6a). $CD4^+$ T helper cells showed increased CD69 and TIM-3 expression, while other tested markers did not show a clear trend (Fig. 4f upper panel). In $CD8^+$ cytotoxic T cells, CD69 and TIM-3 were also significantly upregulated in the presence of CAF. However, CD25, CD137 and PD-1 were significantly down-regulated (Fig. 4f lower panel). These data demonstrated that CAF could impair the activation of T cells and suppress proliferation *in vitro*.

In addition, we analyzed the CAF phenotype after co-culture to evaluate a possible modulation caused by direct T-cell interaction. Strikingly, CAF significantly upregulated VCAM1 as well as the cluster 5 specific CAF protein markers NECTIN2 and CD40 within the three days of co-culture (Fig. 4g), showing that T cells can directly modulate the phenotype of CAF, as implied by spatial proteomics. CD40 is the receptor for T cell activation marker CD154 (CD40L), while NECTIN2 can bind multiple receptors expressed by T cells, suggesting a direct involvement of cluster 5 CAF in the orchestration of T cell responses in CRC.

3.6. NECTIN2 signaling is a central regulator of T cell inhibition by CAF

We hypothesized that CRC CAF can suppress T cell proliferation and activation by upregulating the cluster 5 protein markers NECTIN2 and CD40. To investigate the role of those markers, we applied functional antibodies blocking receptor-ligand binding to co-culture assays. T cell phenotypes were determined based on CD197 (CCR7) and CD45RA expression (Supplementary Fig. 6b) [29,30]. Upon T cell activation, most T cells acquired an effector memory (T_{EM}; approx. 50 % of $CD4^+$ T

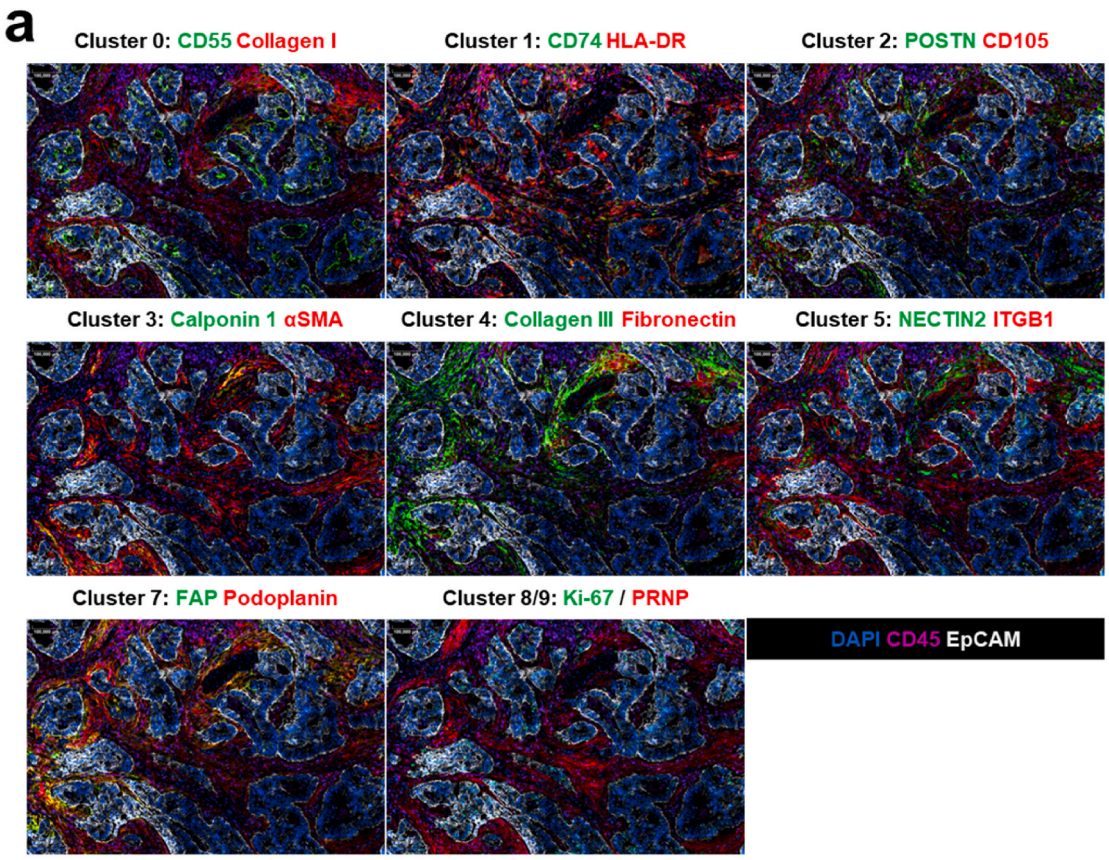

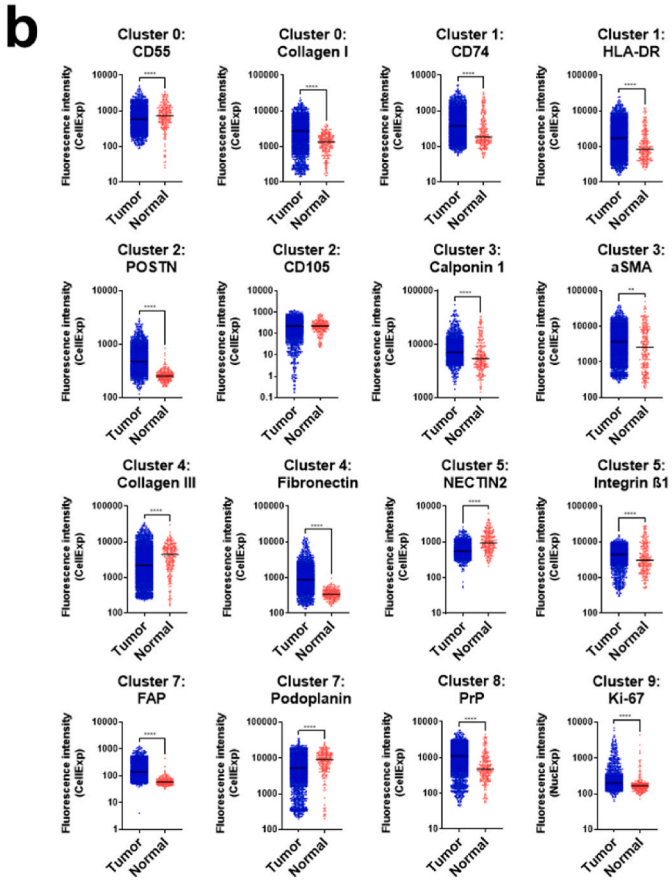

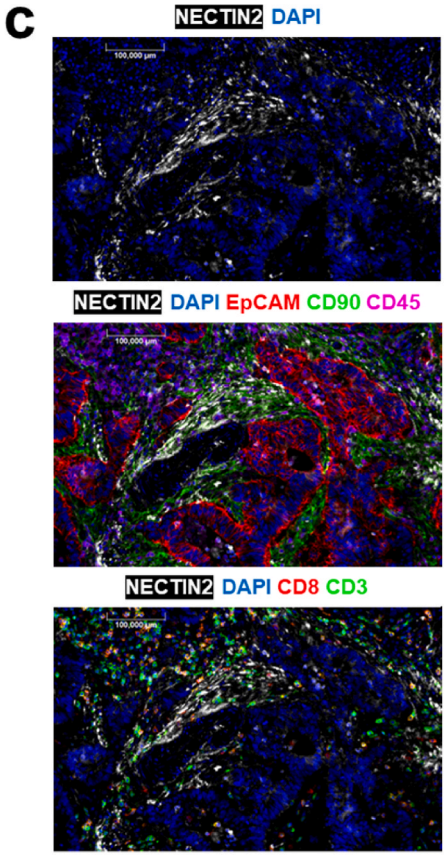

(caption on next page)

Fig. 2. Proteomic analysis to assess the spatial distribution of fibroblast subtypes.
a Selection of 8 cyclic immunofluorescence images of a representative human CRC tissue to evaluate the spatial expression of representative fibroblast cluster marker proteins. **b** Comparison of expression levels (fluorescence intensities; CellExp) of representative fibroblast cluster markers on fibroblasts from one exemplary cyclic immunofluorescence analysis between tumor and normal tissue sections. The figure highlights the overall heterogeneity of markers expressed by fibroblasts in human CRC and colon. Each dot represents expression in one single fibroblast (tumor: n = 2514; normal: n = 251). **c** Representative immunofluorescence images of NECTIN2 staining co-stained with antibodies against epithelial cell marker EPCAM, fibroblast marker CD90, and immune cell marker CD45 in a CRC tissue section. Significance calculated by Mann Whitney tests; lines indicate median (*P < 0.05, **P < 0.01, ***P < 0.001, ****P < 0.0001).

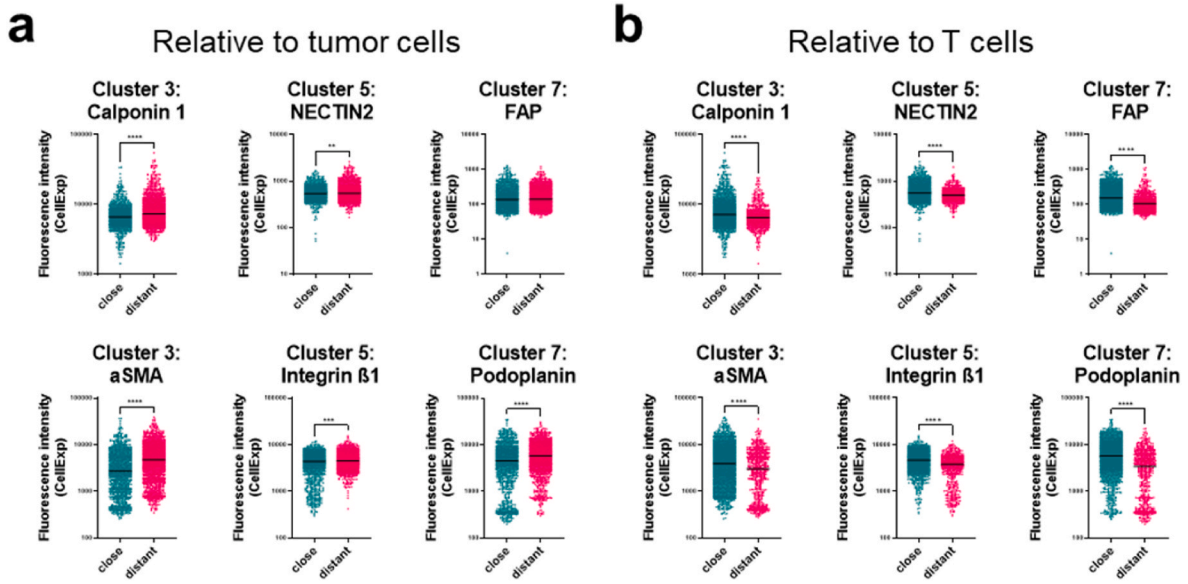

Fig. 3. Influence of cellular neighborhood on CAF marker protein expression.
a Marker expression of CAFs close to EPCAM $^{+}$ cells (<10 μm) vs. CAFs distant from EPCAM^{+} cells (>10 μm, upper panel). Each dot represents an expression in one single CAF (close to EPCAM^{+}: n = 1123; distant from EPCAM^{+}: n = 1391). **b** Marker expression of CAFs close to T cells (<10 μm) vs. CAFs distant from T cells (>10 μm, lower panel). Each dot represents expression in one single CAF (close to T cells: n = 1939; distant from T cells: n = 578).
Significance calculated by Mann Whitney tests; lines indicate median (**P < 0.01, ***P < 0.001, ****P < 0.0001).

cells) or effector memory re-expressing CD45RA phenotype (T_{EMRA} approx. 60 % of CD8^{+} T cells), while only 20–30 % T cells showed a naïve phenotype (Fig. 5a). The direct interaction with CAF significantly reduced the abundance of T_{EM} and T_{EMRA} cells, while approx. 60–80 % of the T cells were retained in the naïve T cell state (T_N). Strikingly, upon antibody-mediated blocking of NECTIN2 but not CD40, the suppressive effect of CAF was completely abrogated, and the phenotypes for CD4^{+} and CD8^{+} T cells resembled the 'T cells only' condition.

Analysis of the activation and exhaustion marker expression on T cells co-cultured with CAF revealed an aberrant phenotype (Fig. 5b): both activation (CD69, CD25) and exhaustion markers (TIM-3, LAG3) were increased compared to T cells alone. In contrast, CD40 and even more pronounced NECTIN2 blockade significantly reduced the expression of CD25, TIM-3, LAG3, and PD1, demonstrating that both CAF markers were required for the suppressive effect. In CD8^{+} T cells, the effects of NECTIN2 blockade were more distinct, suggesting that NECTIN2 is a crucial regulator of CD8^{+} T cell exhaustion. While NECTIN2 blockade showed striking effects on T cell activation and differentiation, the expression of NECTIN2 receptors was not affected (Supplementary Fig. 7a). This was surprising, as CD226 engagement was reported to trigger T cell activation. Moreover, the closely related ligand CD155 (PVR), which can bind the same receptors as NECTIN2, was expressed on CAF as well. Its expression was not affected by the NECTIN2 blockade (Supplementary Fig. 6b), showing that the effects on T cells were indeed predominantly mediated by NECTIN2 rather than CD155.

3.7. *NECTIN2* expression correlates with poor prognosis in CRC patients

To investigate the clinical relevance of cluster 5 CAF-specific gene expression, we evaluated *NECTIN2*, *CD40*, and *CD248* expression in a publicly available clinical database of colon tumors from 1342 patients [27]. Among all colon cancer cases in the database, patients with high *NECTIN2* expression showed a significantly poorer outcome ($p < 0.00005$, HR 1.73) than patients with low *NECTIN2* expression (Fig. 6 upper panel). Similarly, high expression of *CD40* ($p < 0.05$, HR 1.25; Fig. 6 middle) or *CD248* ($p < 0.00005$, HR 1.6; Fig. 6 lower panel) were poor prognostic factors in this patient cohort as well. Given the differences observed in immune infiltration between microsatellite stable (MSS) and microsatellite unstable (MSI) tumors, we expected significant differences between the two groups since MSI tumors typically show a much higher amount of tumor-infiltrating lymphocytes (TILs) [31,32]. High expression of *NECTIN2*, *CD40*, and *CD248* was correlated with a highly significant reduction of relapse-free survival (RFS) only in the 158 MSS patients but not in MSI-high patients (n = 100). There was no difference between tumors in the left or right side of the colon or in patients with and without adjuvant therapy, pointing towards a very general mechanism (Supplementary Fig. 8a). Given the remarkable prognostic value of the cluster 5 CAF marker *NECTIN2*, we tested the correlation of its expression with clinical outcome in other tumor entities. In breast cancer patients, high *NECTIN2* expression was a poor prognostic factor in patients with triple-negative ($p < 0.05$, HR 1.41) and with estrogen and progesterone receptor-negative tumors ($p < 0.05$, HR 1.37), while it was a favorable prognostic factor in the overall population ($p < 5e^{-11}$, HR 0.71; Supplementary Fig. 8b). The protective effect of NECTIN2 in the overall population was surprising, but could potentially be explained by a higher percentage of less aggressive and less inflamed luminal subtypes contributing to the overall population, while the triple-negative and estrogen and progesterone

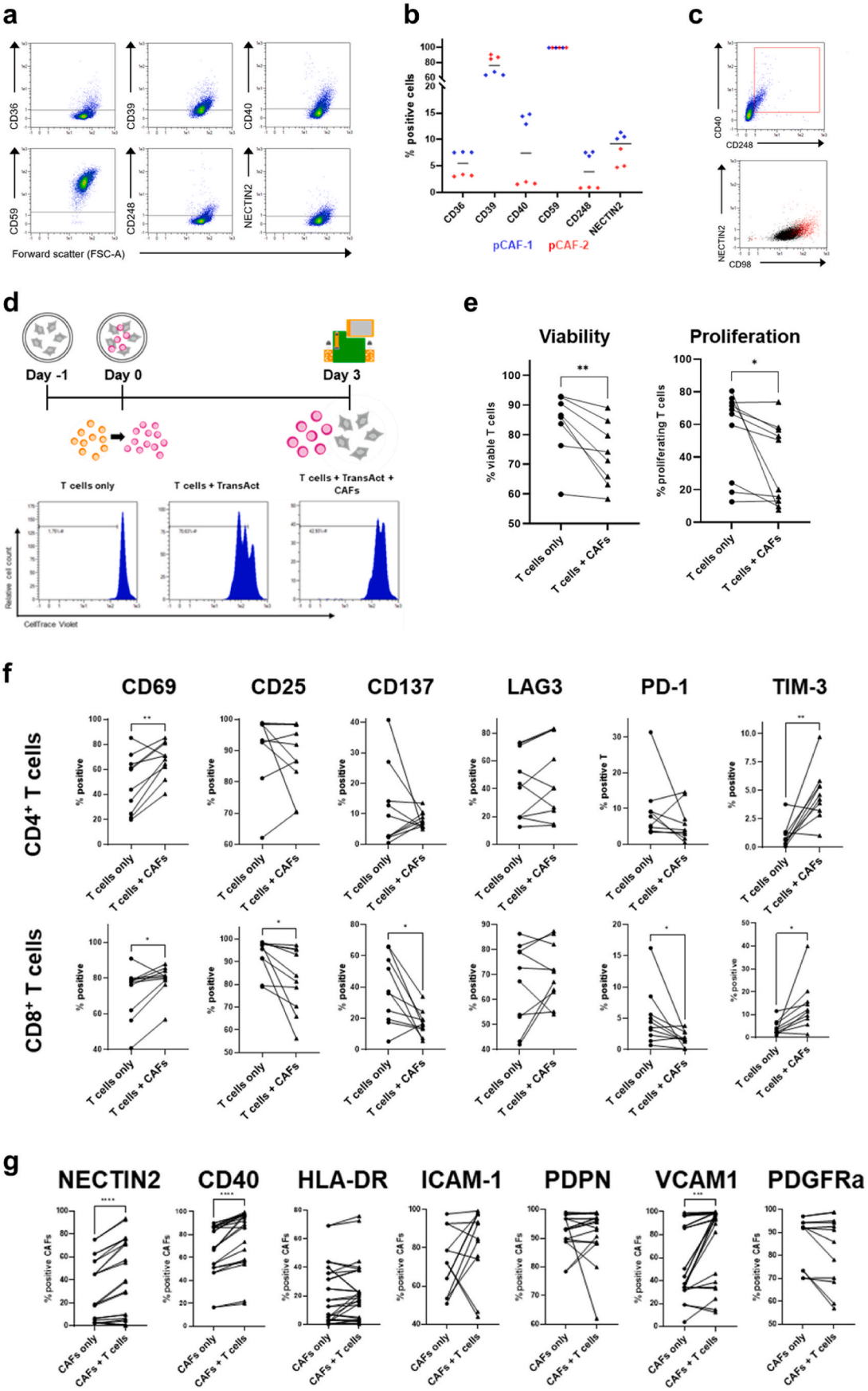

(caption on next page)

Fig. 4. Functional analysis of CAF-T cell interaction.
a Representative density plots from flow cytometric analysis of cluster 5 marker expression in primary CAF cultures (cultured until day 10). **b** Summary of results from two representative primary CAF cultures (n = 3; lines indicate median). **c** Identification of cluster 5 CAF by flow cytometry: CAF were pre-gated on $CD248^{+}CD40^{+}$ double-positive cells (left); these were then shown in a CD98 versus NECTIN2 dotplot in red (right) in comparison to $CD248^{-}CD40^{-}$ CAF (black) from primary cultures (right). **d** Setup of CAF-T cell co-cultures (upper row) and representative histograms demonstrating assessment of T cell proliferation (lower row). **e** Analysis of T cell viability (left; n = 8) and proliferation (right; n = 10) upon co-culture with CAF. **f** Analysis of T cell phenotypes divided into $CD4^{+}$ T cells (upper panel; n = 10) and $CD8^{+}$ T cells (lower panel; n = 10). **g** Assessment of CAF phenotypes after *in vitro* assay (n = 6).
Significance calculated by paired t tests; lines indicate median (*P < 0.05, **P < 0.01, ***P < 0.001, ****P < 0.0001).

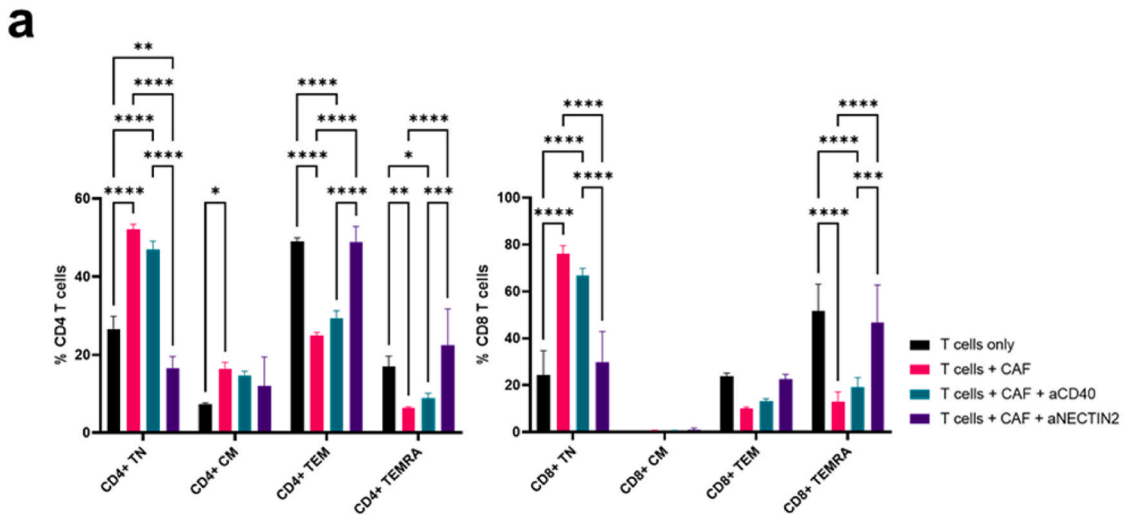

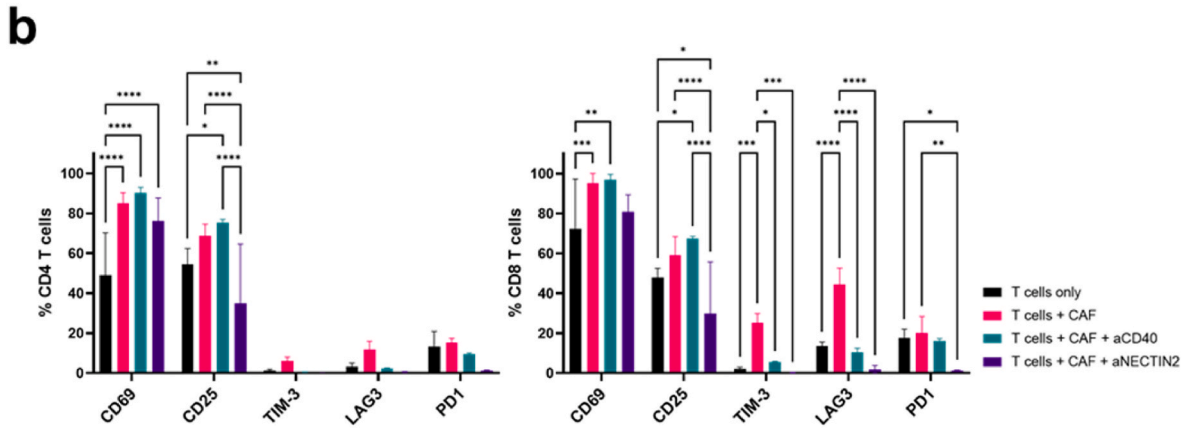

Fig. 5. Blocking of CD40 or NECTIN2 modulates T cell phenotype and exhaustion after co-culture.
a Analysis of $CD4^{+}$ T cell (left) and $CD8^{+}$ T cell (right) phenotypes after co-culture with and without CD40 or NECTIN2 blocking (n = 3). **b** Analysis of activation and exhaustion marker expression on $CD4^{+}$ T cells (left) and $CD8^{+}$ T cells (right) after co-culture with and without CD40 or NECTIN2 blocking (n = 6; two independent experiments). Significance calculated by Two-way ANOVA; data represent mean ± s. e.m. (*P < 0.05, **P < 0.01, ***P < 0.001, ****P < 0.0001).

receptor-negative tumors represent more desmoplastic and aggressive subtypes with high contribution of NECTIN2-positive cells. In patients with pulmonary adenocarcinomas, high *NECTIN2* was correlated with short RFS (p < 0.00005, HR 1.56) (Supplementary Fig. 8b). In gastric cancer (p < 0.01, HR 1.45), as well as in acute myeloid leukemia (AML; p < 0.01, HR 1.17) and multiple myeloma (p < 0.0005, HR 1.45), high *NECTIN2* was a poor prognostic factor as well (Supplementary Fig. 8b). These data highlight the clinical relevance and prognostic value of *NECTIN2* as a potential target for immune therapies.

4. Discussion

This study represents a comprehensive analysis of fibroblast heterogeneity in human colorectal cancer and normal colon tissue from CRC patients, identifying 11 subsets of fibroblasts (Fig. 7a). Among those, previously described subsets, such as myCAF-like, iCAF-like, apCAF-like and "epithelial maintenance" fibroblasts, were found. Four subsets were almost exclusively found in CRC tissue, thus representing CRC CAF. We identified a novel subpopulation of CAF, which we termed T cell-inhibiting CAF (TinCAF) based on its T cell inhibiting and exhaustion-inducing features (Fig. 7b).

Previous studies have focused on CAF heterogeneity and their involvement in immune modulation in the TME, as CAF are the most abundant stromal component in various solid tumors [3,4]. Studies in PDAC highlighted CAF heterogeneity, defining and characterizing widely accepted major subsets such as myCAF, iCAF, and apCAF [15–18]. In this comprehensive study combining transcriptomic and spatial proteomic analyses, we could verify these known subsets in CRC and identify a novel subtype, which we named TinCAF. Of note, in contrast to previous studies in other cancer types, we found apCAF-like fibroblasts in CRC and normal colonic tissue. However, in 2002, Adegboyega and colleagues identified a myofibroblastic fibroblast

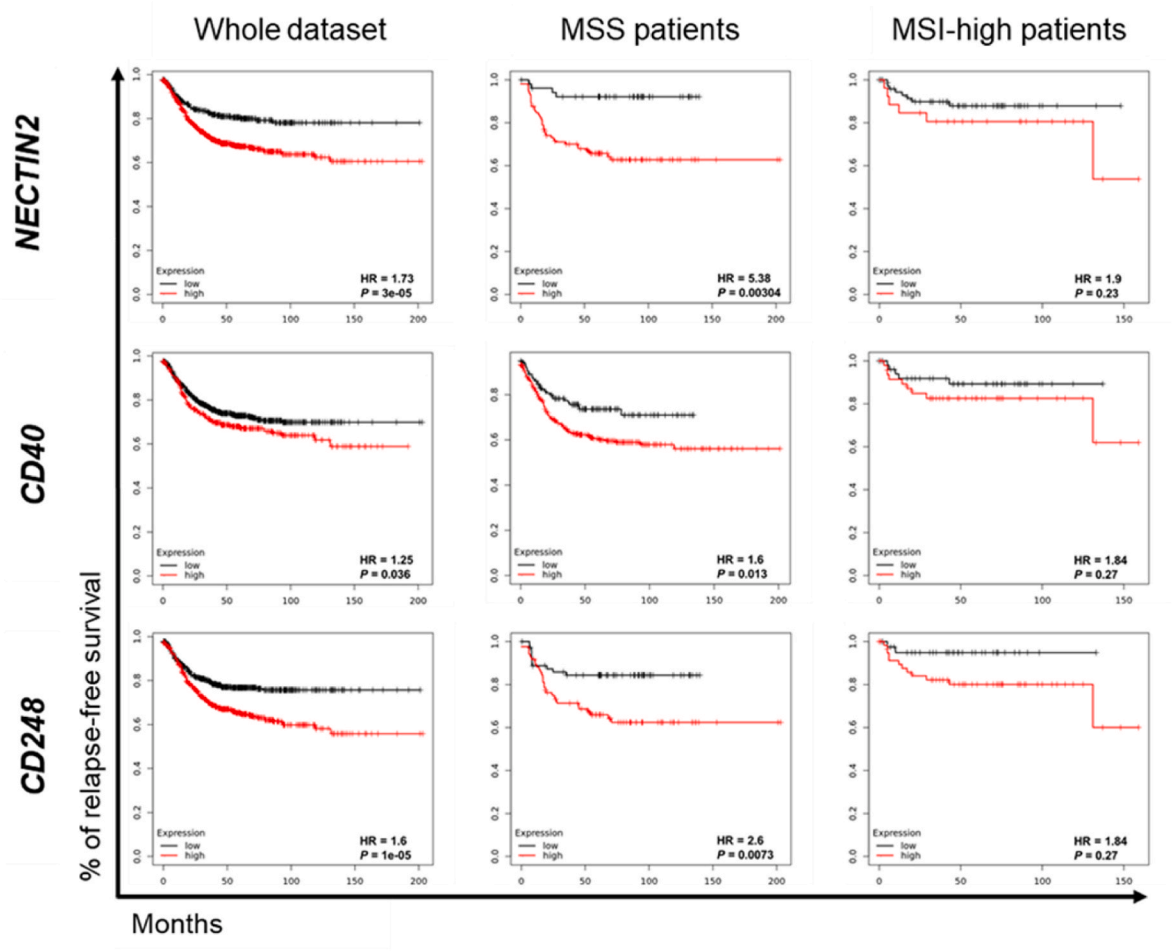

Fig. 6. Clinical significance of cluster 5 CAF markers.
Survival analysis of CRC patients with low (black) versus high (red) *NECTIN2* expression (upper row); low (black) versus high (red) *CD40* expression (middle row); or low (black) versus high (red) *CD248* expression (bottom row).

subpopulation of normal colonic fibroblasts termed pericryptal fibroblasts (PCFs) surrounding the colonic crypts [33]. PCFs have later been shown to express major histocompatibility complex class II and be able to process and present antigens [34]. Hence, the cluster 1 apCAF-like fibroblasts identified in the present dataset most likely represent PCFs from adjacent normal tissue and corresponding apCAF from diseased tissue. The presence of the latter within the cluster was indicated by the analysis of CD74 and HLA-DR expression using spatial proteomics. Both marker proteins were expressed at significantly higher levels in fibroblasts from CRC tissue, showing a cancer-associated increase likely corresponding with the emergence of CAF. This underlines differences in fibroblast biology among different organs, as PCFs are part of the normal colonic environment but are possibly hijacked by cancer cells to contribute to tumor progression.

To validate the expression of characteristic markers for the identified clusters and to analyze their organization and interactions within the tissue, we used spatial proteomics. Interestingly, we found that corresponding protein markers for the CAF clusters were enriched in CAF close to T cells, rather than cancer cells. The effect of immune cells on the emergence and regulation of CAF subpopulations has not been studied in great detail so far, as most studies have focused on CAF-mediated effects on the tumor immune microenvironment [6,7,35–38]. However, our spatial data suggest a close reciprocal interplay between CAF and T cells. Notably, it has been shown that CAF in non-small cell lung cancer can upregulate checkpoint markers PD-L1 and PD-L2 in response to T-cell-secreted interferon gamma [39], demonstrating the direct impact of T cells on CAF phenotypes. Moreover, this study supports our observation of a shift in protein marker expression towards the newly identified TinCAF signature in co-cultures of primary CAF and T cells. It will be interesting to assess whether T cell-derived factors can also fuel other CAF subsets, such as myCAF and iCAF, as this could directly counteract T cell-dependent therapy approaches. This potentially would lead to an increased immunosuppressive and/or -exclusive TME, as suggested in a study that ablated myCAF from the PDAC TME, resulting in increased immunosuppression in the tumor [15].

The role of stromal cells in the constitution of an immunosuppressive environment have now been widely recognized. Most immune suppressive CAF-mediated mechanisms described thus far are exerted via secreted factors such as TGFβ, IL-6 or ECM proteins [6,7,38,40]. Here, we demonstrate a novel T cell-suppressive interaction of TinCAF and T cells mediated via direct NECTIN2 engagement. NECTIN2, a transmembrane glycoprotein with immunoglobulin-like domains that is also known as CD112 or PVRL2 [41,42], has been shown to bind to multiple receptors on T and NK cells, that importantly are also targets of CD155 (PVR) [43,44]. The downstream results of interaction are determined by differential binding affinities of CD155 and NECTIN2 to these receptors [44,45]. However, previous work has mainly focused on the expression of NECTIN2 receptors in immune cells or the expression of CD155 [46–49] rather than the role of NECTIN2 in the stromal compartment of the TME. We found a broad and high expression of CD155 in almost all primary fibroblasts but only a restricted expression of NECTIN2 in the TinCAF subpopulation. Yet, NECTIN2 blocking was sufficient to remove T cell-inhibitory effects. Moreover, NECTIN2 is expressed by CAF but

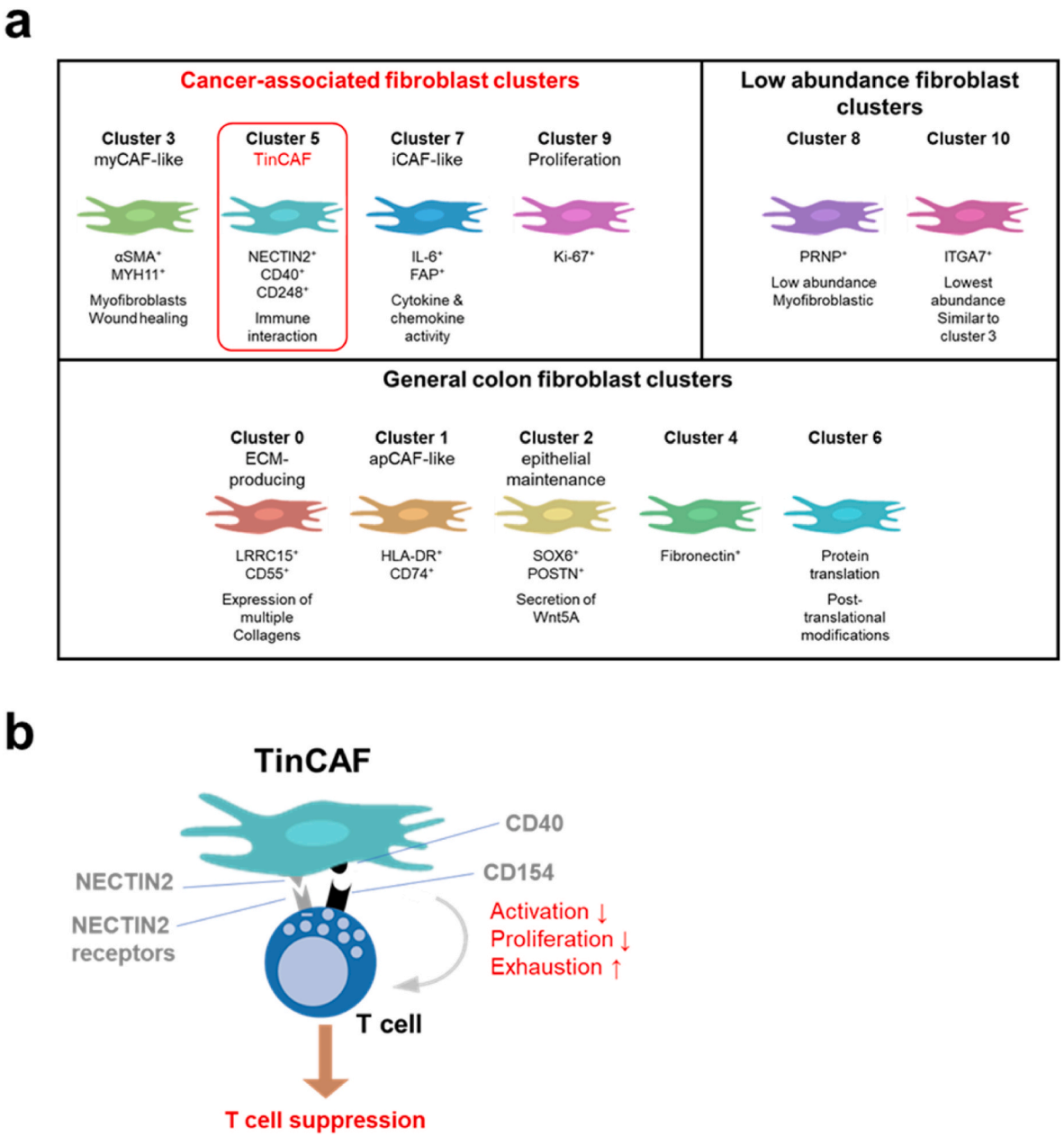

Fig. 7. Summary of fibroblast heterogeneity in colon and CRC.
a Summary of the identified fibroblast clusters. **b** TinCAFs can impair T cell functionality, predominately via NECTIN2 signaling.

not cancer cells, rendering NECTIN2 a key regulator of stromal T cell inhibition. These findings are supported by the work of Murter and colleagues demonstrating that murine $CD8^+$ T cell anti-tumor immunity is significantly impaired upon NECTIN2 engagement and that PVRIG is the primary co-inhibitory T cell receptor [50]. Notably, this study stated that NECTIN2 expression was found in small subsets of myeloid and cancer cells in the CT26 and MC38 subcutaneous mouse colon cancer models used but did not comment on stromal NECTIN2 expression. Our study potentially provides the missing link, as stromal NECTIN2 expression could be the primary regulator in these models next to $NECTIN2^+$ myeloid cells. By genetically manipulating NECTIN2 expression in CAFs, as shown by Ho and colleagues in a model of HCC, the underlying mechanism of NECTIN2 interaction will have to be further explored. The literature about the relevance of NECTIN2 receptor signaling for $CD8^+$ T and NK cell-mediated anti-tumor immunity can explain the poor prognosis for CRC patients with high *NECTIN2* expression. Our study shows that TinCAF are a major source of NECTIN2 expression in CRC.

Immune checkpoint targeting has gained significant attention recently and has led to numerous preclinical and clinical successes in CRC, especially in patients with microsatellite unstable (MSI) tumors [51–53]. In contrast, microsatellite stable (MSS) patients frequently show immune-deserted tumors, rendering immune checkpoint targeting ineffective [53,54]. The CD155-TIGIT axis is an emerging target for immune checkpoint blockade [49,55]. However, we demonstrate that NECTIN2 blockade can override CD155-mediated effects on T cells. NECTIN2 and its receptors could, at least in CRC, be a more promising target for future immune-modulatory therapies. Given that the immunosuppressive TinCAF markers *NECTIN2* and *CD40* are poor prognostic factors, particularly in MSS, blockade of NECTIN2 and CD40 could provide a more MSS-specific immune checkpoint targeting. Nevertheless, despite the remarkable effect of NECTIN2 blocking on T cell functionality, it was not sufficient to restore T cell proliferation. This might be explained by the finding that TinCAF expressed additional

immunomodulatory markers such as CD39 (ENTPD1), CD40, and CD276 (B7–H3). Future studies must show to which extent the additional immunomodulatory molecules expressed by TinCAF constitute the immunosuppressive TME in CRC and how this can be targeted *in vivo*. Suitable *in vivo* models will have to be identified, as the study by Murter and colleagues suggests that murine cell line-induced models of CRC apparently do not show the same restricted NECTIN2 expression on fibroblasts [50] as identified in human samples in the present study.

In summary, we consider this novel NECTIN2-positive CAF subtype a vital player of the suppressive TME and a potential novel target for next-generation immune checkpoint inhibitors. These inhibitors might be a valuable option, especially in MSS tumors where other options for checkpoint inhibition have not shown significant benefits until now.

Data availability

Publicly available data were retrieved via Kaplan-Meier Plotter (https://kmplot.com/analysis/index.php?p=background) [27]. All remaining data are available within the Article, Supplementary information, or available from the authors upon reasonable request.

Code availability

R scripts to read in R environment and the RDS files of the datasets analyzed here are available from the authors upon reasonable request.

CRediT authorship contribution statement

David J. Agorku: Writing – original draft, Visualization, Validation, Project administration, Methodology, Investigation, Formal analysis, Data curation, Conceptualization. **Andreas Bosio:** Writing – review & editing, Supervision, Conceptualization. **Frauke Alves:** Writing – review & editing, Supervision. **Philipp Ströbel:** Writing – review & editing, Supervision. **Olaf Hardt:** Writing – review & editing, Writing – original draft, Supervision, Project administration, Conceptualization.

Declaration of competing interest

The authors declare the following financial interests/personal relationships which may be considered as potential competing interests:

The authors David J. Agorku, Andreas Bosio and Olaf Hardt are employees of Miltenyi Biotec B.V. & Co. KG, while Frauke Alves and Philipp Ströbel declare they have no competing interests.

Acknowledgements

We thank the patients who kindly donated their samples and the contributing surgeons from University Medical Center Göttingen to make this study possible. Moreover, we want to thank Monique Kueffer, Stefan Kueffer, Nojan Jelveh, Christian Wöhle, Anijutta Appelshoffer, Fabio El Yassouri, and Silvia Rüberg for their excellent technical assistance.

Appendix A. Supplementary data

Supplementary data to this article can be found online at https://doi.org/10.1016/j.canlet.2024.216985.

References

[1] J.E.M. Ferlay, F. Lam, M. Colombet, L. Mery, M. Piñeros, A. Znaor, I. Soerjomataram, F. Bray, Global Cancer Observatory: Cancer Today; International Agency for Research on Cancer: Lyon, France. Global Cancer Observatory: Cancer Today, International Agency for Research on Cancer, Lyon, France, 2020.

[2] Y. Ozato, Y. Kojima, Y. Kobayashi, Y. Hisamatsu, T. Toshima, Y. Yonemura, et al., Spatial and single-cell transcriptomics decipher the cellular environment containing HLA-G+ cancer cells and SPP1+ macrophages in colorectal cancer, Cell Rep. 42 (1) (2023) 111929.

[3] R. Kalluri, E. Zeisberg, Controlling angiogenesis in heart valves, Nat. Med. 12 (10) (2006) 1118–1119.

[4] A. Orimo, R.A. Weinberg, Heterogeneity of stromal fibroblasts in tumors, Cancer Biol. Ther. 6 (4) (2007) 618–619.

[5] M. Shimoda, K.T. Mellody, A. Orimo, Carcinoma-associated fibroblasts are a rate-limiting determinant for tumour progression, Semin. Cell Dev. Biol. 21 (1) (2010) 19–25.

[6] R.A. Glabman, P.L. Choyke, N. Sato, Cancer-associated fibroblasts: tumorigenicity and targeting for cancer therapy, Cancers 14 (16) (2022).

[7] R. Mhaidly, F. Mechta-Grigoriou, Role of cancer-associated fibroblast subpopulations in immune infiltration, as a new means of treatment in cancer, Immunol. Rev. 302 (1) (2021) 259–272.

[8] V.S. LeBleu, E.G. Neilson, Origin and functional heterogeneity of fibroblasts, Faseb. J. 34 (3) (2020) 3519–3536.

[9] Y. Kinugasa, T. Matsui, N. Takakura, CD44 expressed on cancer-associated fibroblasts is a functional molecule supporting the stemness and drug resistance of malignant cancer cells in the tumor microenvironment, Stem Cell. 32 (1) (2014) 145–156.

[10] A. Ostman, M. Augsten, Cancer-associated fibroblasts and tumor growth–bystanders turning into key players, Curr. Opin. Genet. Dev. 19 (1) (2009) 67–73.

[11] H. Sugimoto, T.M. Mundel, M.W. Kieran, R. Kalluri, Identification of fibroblast heterogeneity in the tumor microenvironment, Cancer Biol. Ther. 5 (12) (2006) 1640–1646.

[12] R.D. Hofheinz, S.E. al-Batran, F. Hartmann, G. Hartung, D. Jager, C. Renner, et al., Stromal antigen targeting by a humanised monoclonal antibody: an early phase II trial of sibrotuzumab in patients with metastatic colorectal cancer, Onkologie 26 (1) (2003) 44–48.

[13] B.C. Ozdemir, T. Pentcheva-Hoang, J.L. Carstens, X. Zheng, C.C. Wu, T.R. Simpson, et al., Depletion of carcinoma-associated fibroblasts and fibrosis induces immunosuppression and accelerates pancreas cancer with reduced survival, Cancer Cell 25 (6) (2014) 719–734.

[14] A.D. Rhim, P.E. Oberstein, D.H. Thomas, E.T. Mirek, C.F. Palermo, S.A. Sastra, et al., Stromal elements act to restrain, rather than support, pancreatic ductal adenocarcinoma, Cancer Cell 25 (6) (2014) 735–747.

[15] N.G. Steele, G. Biffi, S.B. Kemp, Y. Zhang, D. Drouillard, L. Syu, et al., Inhibition of hedgehog signaling alters fibroblast composition in pancreatic cancer, Clin. Cancer Res. 27 (7) (2021) 2023–2037.

[16] D. Ohlund, A. Handly-Santana, G. Biffi, E. Elyada, A.S. Almeida, M. Ponz-Sarvise, et al., Distinct populations of inflammatory fibroblasts and myofibroblasts in pancreatic cancer, J. Exp. Med. 214 (3) (2017) 579–596.

[17] G. Biffi, T.E. Oni, B. Spielman, Y. Hao, E. Elyada, Y. Park, et al., IL1-Induced JAK/STAT signaling is antagonized by TGFbeta to shape CAF heterogeneity in pancreatic ductal adenocarcinoma, Cancer Discov. 9 (2) (2019) 282–301.

[18] E. Elyada, M. Bolisetty, P. Laise, W.F. Flynn, E.T. Courtois, R.A. Burkhart, et al., Cross-Species single-cell analysis of pancreatic ductal adenocarcinoma reveals antigen-presenting cancer-associated fibroblasts, Cancer Discov. 9 (8) (2019) 1102–1123.

[19] C. Neuzillet, A. Tijeras-Raballand, C. Ragulan, J. Cros, Y. Patil, M. Martinet, et al., Inter- and intra-tumoural heterogeneity in cancer-associated fibroblasts of human pancreatic ductal adenocarcinoma, J. Pathol. 248 (1) (2019) 51–65.

[20] A. Costa, Y. Kieffer, A. Scholer-Dahirel, F. Pelon, B. Bourachot, M. Cardon, et al., Fibroblast heterogeneity and immunosuppressive environment in human breast cancer, Cancer Cell 33 (3) (2018) 463–479 e10.

[21] M. Bartoschek, N. Oskolkov, M. Bocci, J. Lovrot, C. Larsson, M. Sommarin, et al., Spatially and functionally distinct subclasses of breast cancer-associated fibroblasts revealed by single cell RNA sequencing, Nat. Commun. 9 (1) (2018) 5150.

[22] D. Lambrechts, E. Wauters, B. Boeckx, S. Aibar, D. Nittner, O. Burton, et al., Phenotype molding of stromal cells in the lung tumor microenvironment, Nat. Med. 24 (8) (2018) 1277–1289.

[23] L. Zhang, Z. Li, K.M. Skrzypczynska, Q. Fang, W. Zhang, S.A. O'Brien, et al., Single-cell analyses inform mechanisms of myeloid-targeted therapies in colon cancer, Cell 181 (2) (2020) 442–459 e29.

[24] H. Li, E.T. Courtois, D. Sengupta, Y. Tan, K.H. Chen, J.J.L. Goh, et al., Publisher Correction: reference component analysis of single-cell transcriptomes elucidates cellular heterogeneity in human colorectal tumors, Nat. Genet. 55 (1) (2023) 166.

[25] M. Herrera, A. Berral-Gonzalez, I. Lopez-Cade, C. Galindo-Pumarino, S. Bueno-Fortes, M. Martin-Merino, et al., Cancer-associated fibroblast-derived gene signatures determine prognosis in colon cancer patients, Mol. Cancer 20 (1) (2021) 73.

[26] A. Butler, P. Hoffman, P. Smibert, E. Papalexi, R. Satija, Integrating single-cell transcriptomic data across different conditions, technologies, and species, Nat. Biotechnol. 36 (5) (2018) 411–420.

[27] A. Lanczky, B. Gyorffy, Web-based survival analysis tool tailored for medical research (KMplot): development and implementation, J. Med. Internet Res. 23 (7) (2021) e27633.

[28] A. Kinkhabwala, C. Herbel, J. Pankratz, D.A. Yushchenko, S. Ruberg, P. Praveen, et al., MACSima imaging cyclic staining (MICS) technology reveals combinatorial target pairs for CAR T cell treatment of solid tumors, Sci. Rep. 12 (1) (2022) 1911.

[29] F. Sallusto, D. Lenig, R. Forster, M. Lipp, A. Lanzavecchia, Two subsets of memory T lymphocytes with distinct homing potentials and effector functions, Nature 401 (6754) (1999) 708–712.

[30] S. Koch, A. Larbi, E. Derhovanessian, D. Ozcelik, E. Naumova, G. Pawelec, Multiparameter flow cytometric analysis of CD4 and CD8 T cell subsets in young and old people, Immun. Ageing 5 (2008) 6.

[31] J. Bai, H. Chen, X. Bai, Relationship between microsatellite status and immune microenvironment of colorectal cancer and its application to diagnosis and treatment, J. Clin. Lab. Anal. 35 (6) (2021) e23810.
[32] J. Galon, A. Costes, F. Sanchez-Cabo, A. Kirilovsky, B. Mlecnik, C. Lagorce-Pages, et al., Type, density, and location of immune cells within human colorectal tumors predict clinical outcome, Science 313 (5795) (2006) 1960–1964.
[33] P.A. Adegboyega, R.C. Mifflin, J.F. DiMari, J.I. Saada, D.W. Powell, Immunohistochemical study of myofibroblasts in normal colonic mucosa, hyperplastic polyps, and adenomatous colorectal polyps, Arch. Pathol. Lab Med. 126 (7) (2002) 829–836.
[34] J.I. Saada, I.V. Pinchuk, C.A. Barrera, P.A. Adegboyega, G. Suarez, R.C. Mifflin, et al., Subepithelial myofibroblasts are novel nonprofessional APCs in the human colonic mucosa, J. Immunol. 177 (9) (2006) 5968–5979.
[35] M. Sarkar, T. Nguyen, E. Gundre, O. Ogunlusi, M. El-Sobky, B. Giri, et al., Cancer-associated fibroblasts: the chief architect in the tumor microenvironment, Front. Cell Dev. Biol. 11 (2023) 1089068.
[36] S. Guo, J. Yuan, X. Meng, X. Feng, D. Ma, Y. Han, et al., Cancer-associated fibroblasts: just on the opposite side of antitumour immunity? Int. Immunopharm. 122 (2023) 110601.
[37] Y. Chen, K.M. McAndrews, R. Kalluri, Clinical and therapeutic relevance of cancer-associated fibroblasts, Nat. Rev. Clin. Oncol. 18 (12) (2021) 792–804.
[38] D. Lavie, A. Ben-Shmuel, N. Erez, R. Scherz-Shouval, Cancer-associated fibroblasts in the single-cell era, Nat. Can. (Ott.) 3 (7) (2022) 793–807.
[39] R.A. O'Connor, V. Chauhan, L. Mathieson, H. Titmarsh, L. Koppensteiner, I. Young, et al., T cells drive negative feedback mechanisms in cancer associated fibroblasts, promoting expression of co-inhibitory ligands, CD73 and IL-27 in non-small cell lung cancer, OncoImmunology 10 (1) (2021) 1940675.
[40] E. Sahai, I. Astsaturov, E. Cukierman, D.G. DeNardo, M. Egeblad, R.M. Evans, et al., A framework for advancing our understanding of cancer-associated fibroblasts, Nat. Rev. Cancer 20 (3) (2020) 174–186.
[41] F. Eberle, P. Dubreuil, M.G. Mattei, E. Devilard, M. Lopez, The human PRR2 gene, related to the human poliovirus receptor gene (PVR), is the true homolog of the murine MPH gene, Gene 159 (2) (1995) 267–272.
[42] M.S. Warner, R.J. Geraghty, W.M. Martinez, R.I. Montgomery, J.C. Whitbeck, R. Xu, et al., A cell surface protein with herpesvirus entry activity (HveB) confers susceptibility to infection by mutants of herpes simplex virus type 1, herpes simplex virus type 2, and pseudorabies virus, Virology 246 (1) (1998) 179–189.
[43] E.Y. Chiang, I. Mellman, TIGIT-CD226-PVR axis: advancing immune checkpoint blockade for cancer immunotherapy, J Immunother Cancer 10 (4) (2022).
[44] T. Zeng, Y. Cao, T. Jin, Y. Tian, C. Dai, F. Xu, The CD112R/CD112 axis: a breakthrough in cancer immunotherapy, J. Exp. Clin. Cancer Res. 40 (1) (2021) 285.
[45] Y. Zhu, A. Paniccia, A.C. Schulick, W. Chen, M.R. Koenig, J.T. Byers, et al., Identification of CD112R as a novel checkpoint for human T cells, J. Exp. Med. 213 (2) (2016) 167–176.
[46] J.M. Chauvin, H.M. Zarour, TIGIT in cancer immunotherapy, J Immunother Cancer 8 (2) (2020).
[47] B. Sanchez-Correa, I. Valhondo, F. Hassouneh, N. Lopez-Sejas, A. Pera, J. M. Bergua, et al., DNAM-1 and the TIGIT/PVRIG/TACTILE Axis: novel immune checkpoints for natural killer cell-based cancer immunotherapy, Cancers 11 (6) (2019).
[48] H. Stamm, J. Wellbrock, W. Fiedler, Interaction of PVR/PVRL2 with TIGIT/DNAM-1 as a novel immune checkpoint axis and therapeutic target in cancer, Mamm. Genome 29 (11–12) (2018) 694–702.
[49] K. Ducoin, L. Bilonda-Mutala, C. Deleine, R. Oger, E. Duchalais, N. Jouand, et al., Defining the immune checkpoint landscape in human colorectal cancer highlights the relevance of the TIGIT/CD155 Axis for optimizing immunotherapy, Cancers 14 (17) (2022).
[50] B. Murter, X. Pan, E. Ophir, Z. Alteber, M. Azulay, R. Sen, et al., Mouse PVRIG has CD8(+) T cell-specific coinhibitory functions and dampens antitumor immunity, Cancer Immunol. Res. 7 (2) (2019) 244–256.
[51] M. Giannakis, X.J. Mu, S.A. Shukla, Z.R. Qian, O. Cohen, R. Nishihara, et al., Genomic correlates of immune-cell infiltrates in colorectal carcinoma, Cell Rep. 15 (4) (2016) 857–865.
[52] N.J. Llosa, M. Cruise, A. Tam, E.C. Wicks, E.M. Hechenbleikner, J.M. Taube, et al., The vigorous immune microenvironment of microsatellite instable colon cancer is balanced by multiple counter-inhibitory checkpoints, Cancer Discov. 5 (1) (2015) 43–51.
[53] M.M. Germani, R. Moretto, Immune checkpoint inhibitors in mismatch repair proficient/microsatellite stable metastatic colorectal cancer patients: insights from the AtezoTRIBE and MAYA trials, Cancers 14 (1) (2021).
[54] F. Marmorino, A. Boccaccino, M.M. Germani, A. Falcone, C. Cremolini, Immune checkpoint inhibitors in pMMR metastatic colorectal cancer: a tough challenge, Cancers 12 (8) (2020).
[55] Q. Shao, L. Wang, M. Yuan, X. Jin, Z. Chen, C. Wu, TIGIT induces (CD3+) T cell dysfunction in colorectal cancer by inhibiting glucose metabolism, Front. Immunol. 12 (2021) 688961.